

Superconducting and density-wave instabilities of low dimensional conductors with a Zeeman coupling to a magnetic field

M. Shahbazi,¹ Y. Fuseya,² H. Bakrim,¹ A. Sedeki,¹ and C. Bourbonnais¹

¹*Regroupement Québécois sur les Matériaux de Pointe, Département de physique, Université de Sherbrooke, Sherbrooke, Québec, Canada, J1K-2R1,*

²*Department of Engineering Science, University of Electro-Communications, Ch Tokyo 182-8585, Japan*
(Dated: August 4, 2021)

In the framework of the weak coupling renormalization group technique we examine the possible instabilities of the extended quasi-one-dimensional electron gas model with both intrachain and interchain electron-electron interactions, including the influence of umklapp scattering and the coupling of spins to a magnetic field. In the limit of purely repulsive intrachain interactions, we confirm the passage from singlet d -wave like superconductivity to an inhomogeneous FFLO state under magnetic field. The passage is accompanied by an anomalous increase of the upper critical field that scales with the antinesting distance from the quantum critical point joining superconductivity to antiferromagnetism in the phase diagram, as well as the strength of interactions. Adding weak repulsive interchain interactions promotes the passage from singlet to triplet f -wave superconductivity which is expanded under field by the development of a triplet FFLO state with zero angular momentum projection for the Cooper pairs. The connection between theory and experiments on the anomalous upper critical field in the Bechgaard salts is discussed.

PACS numbers: 74.20.Mn, 74.25Dw, 74.70.Kn

I. INTRODUCTION

The $(\text{TMTSF})_2X$ series of organic conductors, also dubbed the Bechgaard salts series, stands out among the first examples of correlated electron systems showing the emergence of superconductivity (SC) following the suppression of a spin-density-wave state (SDW). This is found to occur when either pressure is applied or by chemical means, from anion X substitution.¹⁻³ This proximity has fostered a lot of debate around the nature of the SC order parameter in these materials, and in particular its transformations in magnetic field which will be the main theoretical focus of the present work.

The proximity of SC to SDW in the phase diagram of these quasi-one dimensional (quasi-1D) materials was soon interpreted as a sign of an intimate connection between both ordered states, suggesting that magnetism is directly involved in the development of a SC order parameter. This led to propose that short-range antiferromagnetic fluctuations of the metallic phase, can act as the source of Cooper pairing for electrons⁴⁻⁸. A singlet d -wave (SCd) gap with nodes on the Fermi surface was thus predicted to be the most favourable order parameter for superconductivity, whereas singlet s -wave and triplet p -wave pairings were found to be both suppressed by SDW correlations⁵. This was regarded as consistent with the power law temperature dependence observed in the nuclear spin relaxation rate^{9,10} and the high sensitivity of superconductivity to impurity scattering¹¹⁻¹⁴. However, the singlet d -wave scenario was later on challenged with the puzzling observation in $(\text{TMTSF})_2\text{ClO}_4$ of a thermally activated behaviour of thermal conductivity below T_c ¹⁵, a behaviour that has since been found consistent with the penetration depth extracted from muon spin rotation measurements on the same material¹⁶. When

combined to the aforementioned impurity effect¹⁷, thermal activation may point to a nodeless triplet p -wave SC gap, clearly in conflict with the predictions of microscopic calculations.

On a theoretical basis, the possibility of triplet SC other than p -wave in purely repulsive quasi-1D electron systems has been examined in different ways. From RPA-like approaches¹⁸, it was found that triplet f -wave superconductivity (SCf) can compete with SCd if charge-density-wave (CDW) and SDW fluctuations become of equal importance, a situation that can be reproduced microscopically at sufficiently strong long-range Coulomb interaction along the chains. Such an incursion of SCf besides SCd in the calculated phase diagram of quasi-1D electron gas model was confirmed by the renormalization group (RG) method when the long-range part of the Coulomb term dominates other contributions for purely intrachain interactions¹⁹. When interchain Coulomb interaction is included, even weak in amplitude, it was shown from the RG method that bond centered charge-density wave, also called bond-order (BOW) fluctuations are enhanced besides SDW, which can turn SCd unstable in favor of a SCf triplet ordered state²⁰.

In the interval, the triplet scenario for superconductivity in the Bechgaard salts was further promoted from experiments carried out under magnetic field. This was borne out by a constant and temperature independent NMR Knight shift in the superconducting state of pressurized $(\text{TMTSF})_2\text{PF}_6$ ²¹. The violation from electrical transport measurements of the Glogston criteria or Pauli limit for the critical field of singlet SC was also understood in terms of triplet pairing²²⁻²⁶. Resistivity data show the presence of superconductivity up to a critical field H_{c2}^r standing well above the expected Pauli limiting field H_P known to be bounded by the size of T_c for

singlet Cooper pairing. These experiments were all conducted for field oriented in the ab' plane of highest conduction, an orientation that quenches most of the orbital pair breaking effect, as a result of the strong anisotropy in the electron motion. In these conditions, homogeneous superconductivity can be sustained at arbitrary field if the SC order parameter has a triplet character^{27,28}.

Lower field NMR experiments that were subsequently conducted in $(\text{TMTSF})_2\text{ClO}_4$ modified this view²⁹. They revealed that the Knight shift in the superconducting state is actually suppressed in low field, giving then firm evidence for a singlet SC ground state. However, as the field is increased and crosses some threshold, the Knight shift and nuclear relaxation rate recover their respective normal state values. This arises while superconductivity persists in electrical transport, consistently with the aforementioned violation of the Pauli limit in the ab' plane.

Theoretically, it was proposed from various mean-field approaches that NMR and transport experiments could be reconciled if the SC order parameter experiences a singlet to triplet transition under magnetic field³⁰⁻³⁴. A transition toward a SCf state under field was found to occur using the RG approach to a coupled two-chain version of this problem³⁵. A second possibility put forward in the framework of mean-field theory is a transition toward an inhomogeneous FFLO singlet state under field^{27,28,34,36}, whose conditions of occurrence are particularly optimized for an open quasi-1D Fermi surface. The existence of a field-induced FFLO state in the Bechgaard salts has received a certain empirical support from the observation of an anisotropic onset of the resistive transition in $(\text{TMTSF})_2\text{ClO}_4$ at H_{c2}^r in the ab' plane^{37,38}. Moreover, recent specific heat experiments performed on $(\text{TMTSF})_2\text{ClO}_4$ for similar field orientation^{39,40}, revealed that H_{c2}^r is preceded by a clear thermodynamic signature of the Pauli limit H_P . Besides confirming the singlet nature of the ground state at low field, this critical field scale corresponds to the transition seen by NMR under field.

In a shortened version of the present work, Fuseya *et al.*,⁴¹ examined the field dependence of Cooper pairing from the RG approach to the repulsive quasi-1D electron gas model at incommensurate band filling. The magnetic field was exclusively coupled to spins without pair breaking effects of orbital origin so as to simulate the weakness of the orbital pair breaking for a field oriented in the ab' plane. The calculations revealed that quantum fluctuations linked to the interplay between SDW and SCd have a sizeable impact on the upper critical field H_{c2} . The $H_{c2}(T)$ critical line shows a pronounced upturn at low temperature that largely exceeds the predicted Pauli limit. The difference was found to be non-universal for the ratio $H_{c2}(T)/T_c$, and SCd was shown to become unstable against the formation of a d-wave FFLO (dFFLO) state. No indication for field-induced uniform triplet superconductivity was obtained.

In the present work, we carry on the program of Ref.⁴¹

a step further and extend the RG calculations under magnetic field to the case where half-filling umklapp scattering is present. Umklapp scattering is a key scattering ingredient in systems like the Bechgaard salts which presents some half-filling band character. It is also essential in the quantum criticality associated with the sequence of SDW-SCd instabilities found in these materials^{6,8,42-46}. The instability of SCd against the formation of dFFLO state is confirmed under field, together with its strength correlated to the distance to the quantum critical point along the antinesting axis or the strength of interactions. We also investigate the influence of interchain Coulomb interaction in order to examine if the singlet to triplet transition induced by this interaction is expanded under field. This is found to be the case with the incursion under field of a triplet f -wave FFLO state with zero spin projection for the Cooper pairs, a state that precedes uniform SCf type of superconductivity along the interchain interaction axis.

In Sec. II, we introduce the extended quasi-1D electron gas model and the RG method in the presence of a Zeeman coupling of spins to a magnetic field. In Sec. III, we examine the modification of the phase diagram of the electron gas under magnetic field and the crossover to an inhomogeneous d-wave FFLO in the limit of purely intrachain repulsive interactions. The resulting anomalies in the upper critical field are discussed. In Sec. IV, the influence interchain repulsive interactions on the possible transitions toward triplet superconducting orders under field is investigated. We conclude in Sec. V.

II. THE EXTENDED ELECTRON GAS MODEL IN A MAGNETIC FIELD

A. Model

We consider a linear array of N_P weakly coupled metallic chains of length L , separated by the interchain distance $d_b(\equiv 1)$. The partition function is expressed as a functional integral over the anticommuting $\psi^i s$

$$Z = \int \mathcal{D}\psi^* \mathcal{D}\psi e^{S_0[\psi^*, \psi] + S_I[\psi^*, \psi]}, \quad (1)$$

where the quadratic part of the action is given by

$$S_0[\psi^*, \psi] = \sum_{\mathbf{k}, \sigma} \psi_{p, \sigma}^*(\bar{\mathbf{k}}) [i\omega_n - E_{p, \sigma}(\mathbf{k})] \psi_{p, \sigma}(\bar{\mathbf{k}}), \quad (2)$$

where $\bar{\mathbf{k}} = (\mathbf{k}, \omega_n)$, $\mathbf{k} = (k, k_b)$ is the longitudinal and transverse wave vectors, and ω_n the fermion Matsubara frequencies. The spectrum of the electron gas model, in the presence of a Zeeman coupling of spins to a magnetic field H , takes the form

$$E_{p, \sigma}(\mathbf{k}) = v_F(pk - k_F) + \xi_b(k_b) - \sigma h, \quad (3)$$

where $p = \pm$ refers to right/left moving carriers along the chains of velocity v_F , with k_F as the 1D Fermi wave

vector ($\hbar = 1$ and $k_B = 1$ throughout). Here $h = \mu_B H$ and $\sigma = \pm$ is the spin index. The transverse part of the electron gas spectrum is

$$\xi_b(k_b) = -2t_b \cos k_b - 2t'_b \cos 2k_b, \quad (4)$$

where t_b is the first nearest-neighbours transverse hopping, whereas the second nearest-neighbour hopping $t'_b \ll$

t_b is the antinesting tuning parameter that simulates the main effect of pressure in the model.

In the g-ology picture of interactions, the two-body part of the action can be written in the form

$$\begin{aligned} S_I[\psi^*, \psi] = & -\frac{T}{LN_F} \pi v_F \sum_{\{\bar{k}, \sigma\}} \left\{ g_{\parallel}(\mathbf{k}_{F,1}^-, \mathbf{k}_{F,2}^+, \mathbf{k}_{F,3}^-, \mathbf{k}_{F,4}^+) \psi_{-\sigma}^*(\bar{k}_1) \psi_{+\sigma}^*(\bar{k}_2) \psi_{-\sigma}(\bar{k}_3) \psi_{+\sigma}(\bar{k}_4) \right. \\ & + g_{1\perp}(\mathbf{k}_{F,1}^-, \mathbf{k}_{F,2}^+, \mathbf{k}_{F,3}^-, \mathbf{k}_{F,4}^+) \psi_{-\sigma}^*(\bar{k}_1) \psi_{+,-\sigma}^*(\bar{k}_2) \psi_{-,-\sigma}(\bar{k}_3) \psi_{+,\sigma}(\bar{k}_4) \\ & + g_{2\perp}(\mathbf{k}_{F,1}^+, \mathbf{k}_{F,2}^-, \mathbf{k}_{F,3}^-, \mathbf{k}_{F,4}^+) \psi_{-\sigma}^*(\bar{k}_1) \psi_{+,-\sigma}^*(\bar{k}_2) \psi_{+,-\sigma}(\bar{k}_3) \psi_{-,\sigma}(\bar{k}_4) \\ & \left. + \frac{1}{2} [g_{3\perp}(\mathbf{k}_{F,1}^+, \mathbf{k}_{F,2}^+, \mathbf{k}_{F,3}^-, \mathbf{k}_{F,4}^-) \psi_{+,\sigma}^*(\bar{k}_1) \psi_{+,-\sigma}^*(\bar{k}_2) \psi_{-,-\sigma}(\bar{k}_3) \psi_{-,\sigma}(\bar{k}_4) + \text{c.c.}] \right\} \\ & \times \delta_{\bar{k}_1 + \bar{k}_2, \bar{k}_3 + \bar{k}_4 (\pm \bar{G})}. \end{aligned} \quad (5)$$

The interaction parameters are defined for ingoing and outgoing electrons on the open Fermi surface $\mathbf{k}_F^p(k_b) = (pk_F(k_b), k_b)$ consisting of two ($p = \pm$) sheets parametrized by k_b from the condition $E_p(\mathbf{k}_F^p) = 0$ in zero field. We have in order, the total backscattering amplitude for parallel spins, $g_{\parallel} = g_{1\parallel} - g_{2\parallel}$, which incorporates by exchange a forward scattering contribution; the forward scattering for antiparallel spins, $g_{2\perp}$; and umklapp scattering $g_{3\perp}$ between antiparallel spins for which the longitudinal lattice vector $\bar{G} = (0, 4k_F, 0)$ is involved in momentum conservation. All the couplings are dimensionless and normalized by πv_F .

In the framework of the extended electron gas model^{20,47}, the bare interactions superimpose a purely intrachain contribution and an interchain part between nearest-neighbour chains,

$$\begin{aligned} g_{i,\alpha}(\bar{k}_b) & \equiv g_{i,\alpha}(k_{b1}, k_{b2}, k_{b3}) \\ & = g_{i,\alpha} + 2\mathbf{g}_{i,\alpha} \cos(k_{b1} - k_{b2}), \end{aligned} \quad (6)$$

where $i = 1, 2, 3$ and $\alpha = \parallel, \perp$ for the spins orientation. At the bare level, the transverse momentum dependence is coming solely from the interchain coupling, $\mathbf{g}_{i,\alpha}$, a dependence that is modified on the Fermi surface by the RG flow of the coupling constants.

We will fix the range of the main parameters of the above model in order to simulate the experimental phase diagram of the Bechgaard salts in zero field. From band calculations^{48,49}, we shall take $E_F = v_F k_F = 3000\text{K}$ for typical range of longitudinal Fermi energy and $t_b = 200\text{K}$ for the amplitude of the transverse hopping along the b direction. The antinesting amplitude t'_b of the spectrum

will be kept small compared to t_b and will serve as a tuning parameter to mimic the effect of pressure. As for interactions, although it exists a large range of possible values able to generate a zero field phase diagram compatible with observations for the Bechgaard salts, we can follow the arguments of earlier works to obtain a reasonable set of figures for the intrachain couplings^{20,43-46}. For instance, the bare intrachain backscattering amplitude can be fixed to $g_{1,\alpha} \simeq 0.32$, consistently with the range of values extracted from the enhancement of uniform susceptibility measurements⁵⁰. The presence of a small dimerization gap $\Delta_D \ll E_F$, in the middle of an otherwise three-quarter filled band^{48,49}, leads to weak half-filling umklapp scattering, $g_{3\perp} \approx g_{1\perp} \Delta_D / E_F$ ^{42,51,52}. This gives for umklapp the range of values $g_{3\perp} \approx 0.02 \dots 0.03$. The bare forward scattering amplitude can then be adjusted to $g_{2,\alpha} \simeq 0.64$, so that the calculated temperature scale of the SDW instability from RG at relatively low antinesting falls in the range of observed values $T_{\text{SDW}} \sim 10\text{K}$ for the Bechgaard salts at low pressure². With the above figures, a SDW to SCd sequence of instabilities can be obtained by the RG (e.g., $h = 0$ critical line of Fig. 1 obtained, at $g_{3\perp} = 0.025$), which is compatible with experiments^{2,3}. Finally, regarding the amplitudes of repulsive interchain interaction $\mathbf{g}_{i,\alpha}$, they will be taken variable, but kept small in comparison to their respective intrachain counterparts $g_{i,\alpha}$.

B. Renormalization group equations

We apply a Kadanoff-Wilson RG approach to the extended quasi-1D electron model introduced in the previous subsection. The approach, which has been detailed in previous works^{20,41,44} consists in the perturbative successive partial integrations of electron degrees of freedom in the partition function Z on energy shells of thickness $\Lambda(\ell)d\ell$ at energy distance $\Lambda(\ell) = \Lambda_0 e^{-\ell}$ above and below

$$\begin{aligned}
\partial_\ell g_{\parallel}(\bar{k}_b) &= - \langle g_{\parallel}(\bar{k}_{b1})g_{\parallel}(\bar{k}_{b2})\mathcal{I}_P^0(k_b, q_P) \rangle_{k_b} - \langle g_{1\perp}(\bar{k}_{b1})g_{1\perp}(\bar{k}_{b2})\mathcal{I}_P^{4h}(k_b, q_P) \rangle_{k_b} \\
&\quad + \langle g_{\parallel}(\bar{k}_{b3})g_{\parallel}(\bar{k}_{b2})\mathcal{I}_C^0(k_b, q_C) \rangle_{k_b} - \langle g_{3\perp}(\bar{k}_{b1})g_{3\perp}(\bar{k}_{b2})\mathcal{I}_P^{4h}(k_b, -q_P) \rangle_{k_b} \\
\partial_\ell g_{1\perp}(\bar{k}_b) &= - \langle [g_{\parallel}(\bar{k}_{b1})g_{1b}(\bar{k}_{b2}) + g_{\parallel}(\bar{k}_{b2})g_{1\perp}(\bar{k}_{b3})] (\mathcal{I}_P^0(k_b, -q_{bP}) + \mathcal{I}_P^{4h}(k_b, -q_P)) / 2 \rangle_{k_b} \\
&\quad + \langle [g_{2\perp}(\bar{k}_{b3})g_{1\perp}(\bar{k}_{b1}) + g_{2\perp}(\bar{k}_{b4})g_{1\perp}(\beta_{b1})] (\mathcal{I}_C^{4h}(k_b, q_{bC}) + \mathcal{I}_C^0(k_b, q_C)) / 2 \rangle_{k_b}, \\
\partial_\ell g_{2\perp}(\bar{k}_b) &= - \langle g_{1\perp}(\bar{k}_{b3})g_{1\perp}(\bar{k}_{b4})\mathcal{I}_C^{4h}(k_b, q_C) \rangle_{k_b} + \langle g_{2\perp}(\bar{k}_{b3})g_{2\perp}(\bar{k}_{b4})\mathcal{I}_C^0(k_b, q_C) \rangle_{k_b} \\
&\quad - \langle [g_{2\perp}(\bar{k}_{b1})g_{2\perp}(\bar{k}_{b3}) + g_{3\perp}(\bar{k}_{b1})g_{3\perp}(\bar{k}_{b2})] \mathcal{I}_P^0(k_b, -q_P) \rangle_{k_b}, \\
\partial_\ell g_{3\perp}(\bar{k}_b) &= - \langle g_{\parallel}(\bar{k}_{b1})g_{3\perp}(\bar{k}_{b2}) (\mathcal{I}_P^0(k_b, q_P) + \mathcal{I}_P^{4h}(k_b, q_P)) / 2 \rangle_{k_b} \\
&\quad + \langle g_{\parallel}(\bar{k}_{b2})g_{3\perp}(\bar{k}_{b1}) (\mathcal{I}_P^{4h}(k_b, -q_P) + \mathcal{I}_P^0(k_b, -q_P)) / 2 \rangle_{k_b} \\
&\quad - \langle g_{2\perp}(\bar{k}_{b5})g_{3\perp}(\bar{k}_{b6})\mathcal{I}_P^0(k_b, q'_P) + g_{2\perp}(\bar{k}_{b5})g_{3\perp}(\bar{k}_{b6})\mathcal{I}_P^0(k_b, -q'_P) \rangle_{k_b}, \tag{7}
\end{aligned}$$

where $\langle \dots \rangle_{k_b} = 1/N_P \sum_{k_b} \dots$ and

$$\begin{aligned}
\bar{k}_{b1} &= (k_b, k_{b4}, k_{b1}) \\
\bar{k}_{b2} &= (k_b, k_{b2}, k_{b3}) \\
\bar{k}_{b3} &= (k_{b1}, k_{b2}, k_b) \\
\bar{k}_{b4} &= (k_{b3}, k_{b4}, k_b) \\
\bar{k}_{b5} &= (k_b, k_{b4}, k_{b2}) \\
\bar{k}_{b6} &= (k_{b1}, k_b, k_{b3})
\end{aligned}$$

$q_P^{(\nu)} = k_{b3} - k_{b2,1} = k_{b1,2} - k_{b4}$ and $q_C = k_{b1,3} + k_{b2,4}$. The on-shell Peierls ($\nu = P$) and Cooper ($\nu = C$) loops at finite T and h are given by

$$\begin{aligned}
\mathcal{I}_\nu^{\kappa h}(k_b, q_\nu^{(\nu)}) &= \frac{\Lambda(\ell)}{2} \sum_{\lambda=\pm 1} \int_{k_b - \frac{\pi}{N_P}}^{k_b + \frac{\pi}{N_P}} \frac{dk_b}{2\pi} \\
&\quad \times \frac{\theta(|\Lambda(\ell) + \lambda A_\nu^{\kappa h}| - \Lambda(\ell))}{2\Lambda(\ell) + \lambda A_\nu^{\mu h}} \\
&\quad \times \left[\tanh[\beta\Lambda(\ell)/2] + \tanh[\beta(\Lambda(\ell)/2 + \lambda A_\nu^{\kappa h}/2)] \right], \tag{8}
\end{aligned}$$

where for the loop field dependence, $\kappa = 0, 4$. Here $\theta(x)$

the Fermi surface, where $\Lambda_0 \equiv E_F$ is the initial cutoff fixed at the Fermi energy. Each energy shell is divided into N_P patches, in which a transverse momentum integration is carried out for the internal variables of the logarithmically singular electron-electron (Copper) and electron-hole (Peierls) loops of the scattering channels.

At the one-loop level, the RG flow equations for the 3-momentum dependent scattering amplitudes $g_{i,\alpha}$ at non zero magnetic field are

is the Heaviside function [$\theta(0) \equiv \frac{1}{2}$], and

$$\begin{aligned}
A_\nu^{\kappa h}(k_b, q_\nu^{(\nu)}) &= -\xi_b(k_b) - \eta_\nu \xi_b(\eta_\nu k_b + q_\nu^{(\nu)}) \\
&\quad + \eta_\nu \xi_b(\eta_\nu k_{b2(4)} + q_\nu^{(\nu)}) + \xi_b(k_{b2(4)}) + \kappa h, \tag{9}
\end{aligned}$$

for which $\eta_{P,C} = \pm 1$.

To find out the nature of instabilities of the electron system, we compute the susceptibilities associated with the different possibilities of staggered density-wave and Cooper pairing correlations. Under successive partial integrations of the RG transformation, the linear coupling of pair of carriers to an external source field h_μ in the correlation channel μ , yields the generic expression of the normalized temperature dependent susceptibility ($\tilde{\chi}_\mu = \pi \nu_F \chi_\mu$) at the wave vector \mathbf{q}_μ :

$$\tilde{\chi}_\mu(\mathbf{q}_\mu) = 2 \int_0^\infty \langle z_\mu^2(k_b) \mathcal{I}_\mu^{\kappa h}(k_b, q_\mu) \rangle_{k_b} d\ell, \tag{10}$$

where $z_\mu(k_b)$ is the renormalization factor for the source-pair vertex. It obeys the flow equation

$$\partial_\ell z_\mu(k_b) = \frac{1}{2} \langle f_\mu(k'_b) g_\mu(\bar{k}'_b) \mathcal{I}_\mu^{\kappa h}(k'_b, q_\mu) \rangle_{k'_b}, \tag{11}$$

where g_μ is a momentum dependent combination of couplings for the correlation of the channel μ and $f_\mu(k_b)$ is

a form factor associated with the nature of correlations.

If we first look at the density-wave susceptibilities for which $f_\mu = 1$, we have in the charge sector, the site-centred ($\mu = \text{CDW}$) and bond-centred ($\mu = \text{BOW}$) charge-density wave susceptibilities, corresponding to the following combinations of couplings at the modulation (nesting) wave vector $\mathbf{q}_{\text{CDW}} = \mathbf{q}_{\text{BOW}} = (2k_F, \pi)$,

$$g_\mu \mathcal{I}_\mu^{\kappa\mu h} \Big|_{\mu=\text{CDW,BOW}} = -[g_{1\perp}(k'_b + \pi, k_b, k_b + \pi) + g_{\parallel}(k'_b + \pi, k_b, k_b + \pi) \pm g_{3\perp}(k'_b + \pi, k_b + \pi, k_b)] \mathcal{I}_P^{2h}(k'_b, \pi). \quad (12)$$

In the spin sector, the site-centred SDW susceptibility is likely to become singular. In presence of a magnetic field along z , the rotational symmetry is broken, which splits this susceptibility into longitudinal ($\tilde{\chi}_{\text{SDW}_z}$) and transverse ($\tilde{\chi}_{\text{SDW}_{xy}}$) components for which,

$$g_\mu \mathcal{I}_\mu^{\kappa\mu h} \Big|_{\mu=\text{SDW}_z, \text{SDW}_{xy}} = [g_{2\perp}(k'_b + \pi, k_b, k_b + \pi) + g_{3\perp}(k'_b + \pi, k_b + \pi, k'_b)] \mathcal{I}_P^{2h,0}(k'_b, \pi) \quad (13)$$

If we consider in the second place the SC susceptibilities at $\mathbf{q}_\mu = 0$ that may be potentially singular in the presence of a magnetic field, we have for the singlet SC channel,

$$f_\mu g_\mu \mathcal{I}_\mu^{\kappa\mu h} = -f_\mu(k'_b) [g_{1\perp}(k'_b, -k'_b, k_b) + g_{2\perp}(k'_b, -k'_b, k_b)] \mathcal{I}_C^{2h}(k'_b, 0). \quad (14)$$

For singlet s -wave susceptibility, $\tilde{\chi}_{\text{SS}}, f_{\text{SS}} = 1$; for d -wave susceptibility, $\tilde{\chi}_{\text{SCd}}, f_{\text{SCd}}(k_b) = \sqrt{2} \cos k_b$; for g -wave, $\tilde{\chi}_{\text{SCg}}, f_{\text{SCg}} = \sqrt{2} \cos 2k_b$, etc.

For the triplet channel at $\mathbf{q}_\mu = 0$, the SC susceptibilities are governed by the expressions

$$f_\mu g_\mu \mathcal{I}_\mu^{\kappa\mu h} = f_\mu(k'_b) [g_{1\perp}(k'_b, -k'_b, k_b) - g_{2\perp}(k'_b, -k'_b, k_b)] \mathcal{I}_C^{2h}(k'_b, 0), \quad (15)$$

for antiparallel spins at $S_z = 0$, whereas for parallel spins at $S_z = \pm 1$,

$$f_\mu g_\mu \mathcal{I}_\mu^{\kappa\mu h} = f_\mu(k'_b) g_{\parallel}(k'_b, -k'_b, k_b) \mathcal{I}_C^0(k'_b, 0), \quad (16)$$

For both cases, we have for p -wave susceptibility, $\tilde{\chi}_{\text{SCP}}, f_{\text{SCP}} = 1$; f -wave $\tilde{\chi}_{\text{SCf}}, f_{\text{SCf}} = \sqrt{2} \cos k_b$; etc.

Now for superconductivity, it is possible for electrons of opposite spins to form Cooper pairs with a nonzero momentum $\mathbf{q}_h = (2h/v_F, 0)$ in a FFLO state. This case requires a separate treatment of the pair vertex z_μ ⁴¹, which actually splits into $z_\mu^{\uparrow\downarrow}$ and $z_\mu^{\downarrow\uparrow}$ for opposite spins. For singlet FFLO, these are governed by

$$\begin{aligned} \partial_\ell z_\mu^{\uparrow\downarrow(\downarrow\uparrow)}(k_b) = & - \left\langle f_\mu(k'_b) [g_{1\perp}(-k'_b, k'_b, -k_b) z_\mu^{\downarrow\uparrow(\uparrow\downarrow)}(k'_b) \right. \\ & \times \mathcal{I}_C^{0(4h)}(k'_b, 0) + g_{2\perp}(-k'_b, k'_b, -k_b) z_\mu^{\uparrow\downarrow(\downarrow\uparrow)}(k'_b) \\ & \left. \times \mathcal{I}_C^{4h(0)}(k'_b, 0)] \right\rangle_{k'_b}, \end{aligned} \quad (17)$$

where for s -wave FFLO, $f_{\text{sFFLO}} = 1$; d -wave FFLO, $f_{\text{dFFLO}}(k_b) = \sqrt{2} \cos k_b$; etc.

It is also possible in principle for triplet Cooper pairing with zero total spin projection, $S_z = 0$, to develop an inhomogeneous FFLO state following the equations

$$\begin{aligned} \partial_\ell z_\mu^{\uparrow\downarrow(\downarrow\uparrow)}(k_b) = & \left\langle f_\mu(k'_b) [g_{1\perp}(-k'_b, k'_b, -k_b) z_\mu^{\downarrow\uparrow(\uparrow\downarrow)}(k'_b) \right. \\ & \times \mathcal{I}_C^{0(4h)}(k'_b, 0) - g_{2\perp}(-k'_b, k'_b, -k_b) z_\mu^{\uparrow\downarrow(\downarrow\uparrow)}(k'_b) \\ & \left. \times \mathcal{I}_C^{4h(0)}(k'_b, 0)] \right\rangle_{k'_b}, \end{aligned} \quad (18)$$

where for $S_z = 0$ of p -wave, $f_{\text{pFFLO}} = 1$; f -wave, $f_{\text{fFFLO}} = \sqrt{2} \cos k_b$; etc.

The corresponding temperature dependent susceptibilities for the whole set of FFLO states take the following form

$$\begin{aligned} \tilde{\chi}_\mu(\mathbf{q}_h) = & \int_0^\infty \langle [z_\mu^{\uparrow\downarrow}(k_b)]^2 \mathcal{I}_{C\ell}^0(k_b, 0) \\ & + [z_\mu^{\downarrow\uparrow}(k_b)]^2 \mathcal{I}_{C\ell}^{4h}(k_b, 0) \rangle_{k_b} d\ell. \end{aligned} \quad (19)$$

III. RESULTS FOR THE MODEL WITH INTRACHAIN INTERACTIONS

We first examine the results of integration of the above RG equations for $\mathbf{g}_{i,\alpha} = 0$ in Eq. (6), namely when only intrachain interactions are present. In zero magnetic field the sequence of instabilities obtained for the input parameters of model given in Sec. II A coincides with the one found in previous works^{45,46}. Thus, at relatively low antinesting amplitude t'_b , a singularity in $\tilde{\chi}_{\text{SDW}}$ at $\mathbf{q}_{\text{SDW}} = (2k_F, \pi)$ is found from (10) and (13). The critical temperature T_{SDW} is traced in Fig. 1, which decreases monotonically by increasing t'_b . Close to the critical value t'_b^* ($\simeq 32\text{K}$, $t'_b^*/t_b \simeq 0.16$), T_{SDW} drops rapidly until t'_b^* is reached and the system becomes unstable against the formation of a SCd state, with the divergence of $\tilde{\chi}_{\text{SCd}}$ coming from the singularity of (14) at a maximum $T_c \sim 1\text{K}$ [See Fig. 2 (a)]; T_c then closes the sequence by its steady decrease with $t'_b > t'_b^*$, as shown in Fig. 1. The typical momentum profile of the SC combination of couplings $g_{\text{SCd}}(k'_b, -k'_b, k_b)$ in the $k_b k'_b$ plane for temperature close to T_c , plane shows pronounced modulations compatible with the form factor f_{SCd} for SCd superconductivity. According to Fig. 3 (b), this modulation in momentum space is intimately connected with the amplitude and anisotropy developed by umklapp, $g_{3\perp}(k'_b, -k'_b, k_b)$, along the lines $k'_b = \pm k_b \pm \pi$, and which from (13), is directly involved in the strength of SDW correlations responsible for SCd pairing.

For non zero magnetic field, the SDW instability at low t'_b is now taken place for spins oriented in the xy plane transverse to the field. The amplitude of T_{SDW} obtained in Fig. 1 is slightly reinforced compared to zero field. This reinforcement of antiferromagnetism agrees

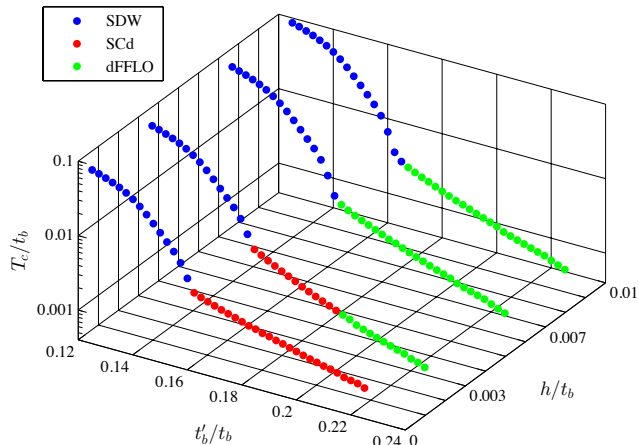


FIG. 1. The phase diagram of the quasi-1D electron gas model with intrachain interactions as a function of magnetic field.

with an increase of the critical t'_b^* with h . At very low field, this presents as an increase of the maximum SCd T_c with h , which is possible because orbital pair breaking is absent from the model. However, the SDW \rightarrow SCd sequence of instabilities is rapidly altered under field. As shown in Fig. 1, where an incursion of a dFFLO instability takes place along the antineesting axis, as signalled by a singularity of $\tilde{\chi}_{\text{dFFLO}}(\mathbf{q}_h)$ coming from (17) at a nonzero pairing momentum $\mathbf{q}_h = (2h/v_F, 0)$. The related divergence occurs at a T_c that is steadily suppressed under field, but whose amplitude is significantly enhanced compared to mean-field calculations in which the interplay between the Cooper and density-wave pairing is neglected^{34,41}. From Fig. 3 (c), the combination of couplings $g_{1\perp}(k'_b, -k'_b, k_b) + g_{2\perp}(k'_b, -k'_b, k_b)$ entering in (17) for singlet FFLO superconductivity presents also d-wave like modulations in the $k_b k'_b$ plane, but of weaker amplitude compared to the zero field situation.

Regarding triplet superconductivity, we see from Fig. 2 (a) that apart from a regular enhancement of χ_{SCf} at low temperature no crossover to triplet superconductivity is found under field when only intrachain interactions are present. This result differs from the mean-field phenomenology when both singlet and triplet pairing interactions are present^{30–32}

A. H - T phase diagram

In the superconducting sector of the phase diagram of Fig. 1, one can follow the critical temperature $T_c(h)$ with field, or conversely the upper critical field profile $h_{c2}(T)$ with temperature of Fig. 4. At very low field, the slope dh_{c2}/dT is at first positive, indicating that T_c increases with h . This results from the strengthening of SDW correlations, which as the source of Cooper pair-

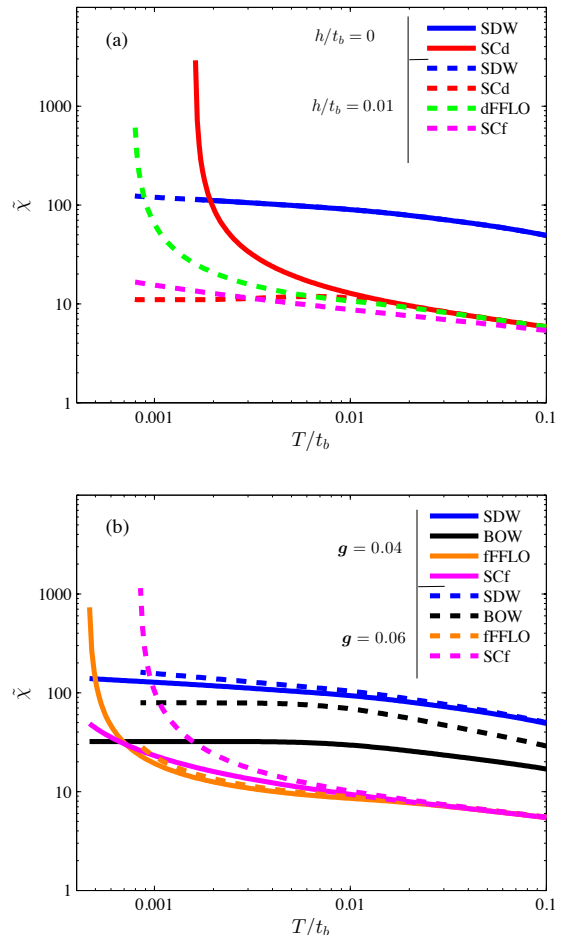


FIG. 2. Temperature dependence of the susceptibilities in the normal phase of the superconducting sector of the phase diagram at $t'_b/t_b = 0.21$. (a): For intrachain couplings only, $g_i = 0$ at zero and finite magnetic fields. (b): For finite interchain couplings $g_i \neq 0$ at $h/t_b = 0.01$.

ing in the SCd channel, exceeds the field pair breaking effect on the singlet state in (10) and (14). As previously mentioned, this enhancement of T_c takes place because orbital effect caused by the field is absent in the present model. At higher field, however, singlet pair breaking dominates and T_c decreases, as shown in Fig. 4. The values of h_{c2} are systematically above the mean-field result for the pure Pauli limit (dashed lines of Fig. 4)⁵³. Instead of extrapolating to a field close to h_P in the low temperature limit, h_{c2} continues until a crossover to an inhomogeneous dFFLO state is achieved. In the dFFLO regime, h_{c2} not only exceeds the Pauli limiting field $h_P (\simeq 1.25T_c)$, but also the Pauli limit of FFLO state for isotropic 2D ($h_P \simeq 1.78T_c$) and 3D ($h_P \simeq 1.34T_c$) superconductors⁵³.

Another important feature of the present results⁴¹, which contrasts with mean-field type of calculations, is the non-universality of the ratio h_{c2}/T_c , as a function of either the antineesting amplitude t'_b [Fig. 4 (a)] or inter-

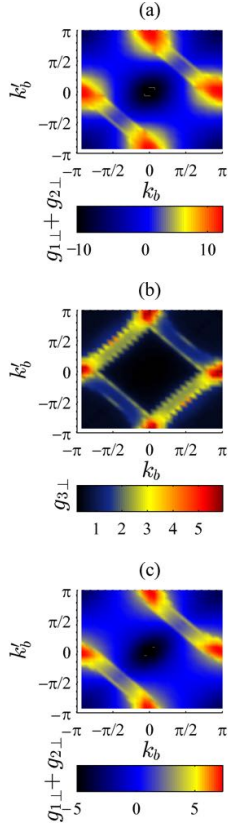


FIG. 3. Low temperature renormalized effective scattering amplitudes at $t'_b/t_b = 0.21$ for singlet Cooper pairing $g_{1\perp}(k'_b, -k'_b, k_b) + g_{2\perp}(k'_b, -k'_b, k_b)$ in the k_b, k'_b plane for the normal phase of (a) : SCd ($h = 0$); (b): umklapp amplitude $g_{3\perp}(k'_b, -k'_b, k_b)$ at $h = 0$; (c) : dFFLO ($h/t_b = 0.01$).

action [e.g., $g_{3\perp}$, in Fig. 4 (b)]. At the root of this lack of universality stands SDW fluctuations as the source of Cooper pairing. In this respect, the RG flow equations (7) tell us that, in contrast to mean-field theory, the coupling components defining the effective singlet pairing interaction $g_{1\perp} + g_{2\perp}$ entering in $\tilde{\chi}_{\text{dFFLO}}$ from (17), are continuously altered by SDW correlations in the course of decreasing $\Lambda(\ell)$ (See also Fig. 3). The initial values of couplings or antineesting modify this energy scale dependent interference effect. This indicates that in practice, the observation of the lack of universality in the anomalous upper critical field, as a function of the applied pressure in the Bechgaard salts for instance, would be a distinctive signature of fluctuation induced unconventional pairing in the material⁴¹. On experimental side, there are some indications that this is indeed the case⁵⁴.

IV. INTERCHAIN INTERACTIONS

We now turn to the influence of interchain electron-electron repulsive interactions introducing a non zero $\mathbf{g}_{i,\alpha}$ in the interaction parameters (6) of the extended quasi-

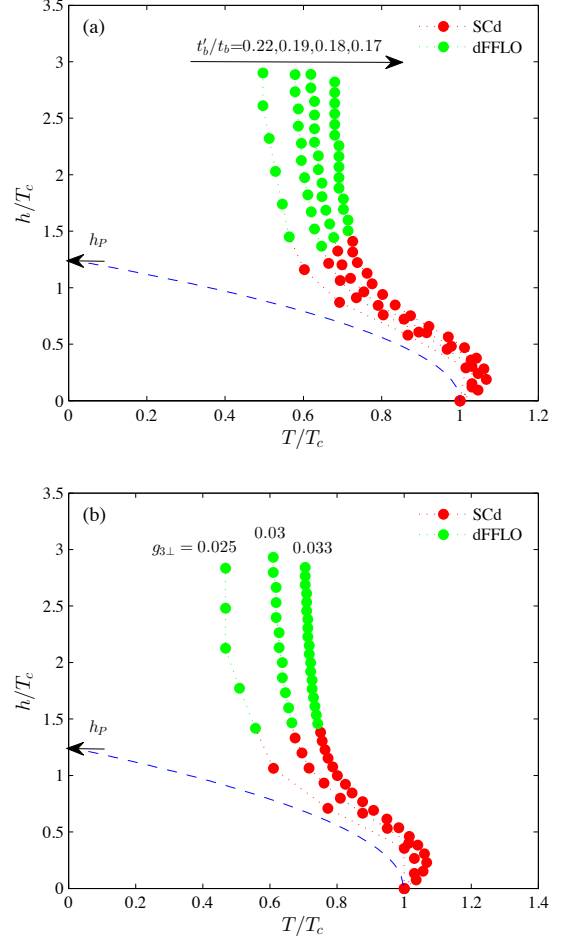


FIG. 4. The variation of the normalized upper critical field h_{c2}/T_c with temperature for (a) : various t'_b and (b) : different amplitudes of umklapp scattering $g_{3\perp}$ at $t'_b/t_b = 0.22$. The dashed line is mean-field result for the upper critical field in the Pauli limit.

1D electron gas model^{20,47}. We shall take for simplicity the transverse backward and forward scattering amplitudes equal by putting, $\mathbf{g}_{1,\alpha} = \mathbf{g}_{2,\alpha} \equiv \mathbf{g}$, for both parallel ($\alpha = \parallel$) and perpendicular ($\alpha = \perp$) spins. As for the transverse umklapp amplitude, we have the following ratio with backward scattering, $\mathbf{g}_{3\perp}/\mathbf{g} = g_{3\perp}/g_{1\perp}$, which is the same as for intrachain interactions discussed in Sec. III A.

We first review the case in zero magnetic field, which was examined by Nickel *et al.*²⁰. By increasing the amplitude of \mathbf{g} , the SDW \rightarrow SCd sequence of instabilities tuned by t'_b is modified from the relatively small value, $\mathbf{g} \simeq 0.04$, of interchain repulsion. According to Fig. 5 (a), a triplet f -wave instability in $\tilde{\chi}_{\text{SCf}}$ of (15-16) gets into the sequence that becomes SDW \rightarrow SCd \rightarrow SCf. By increasing \mathbf{g} , it transforms into SDW \rightarrow SCf, where SDW is connected directly to SCf at the quantum critical point t'_b^* . The emergence of SCf state emerges from the rise of BOW fluctuations which are detrimental to singlet SCd pair-

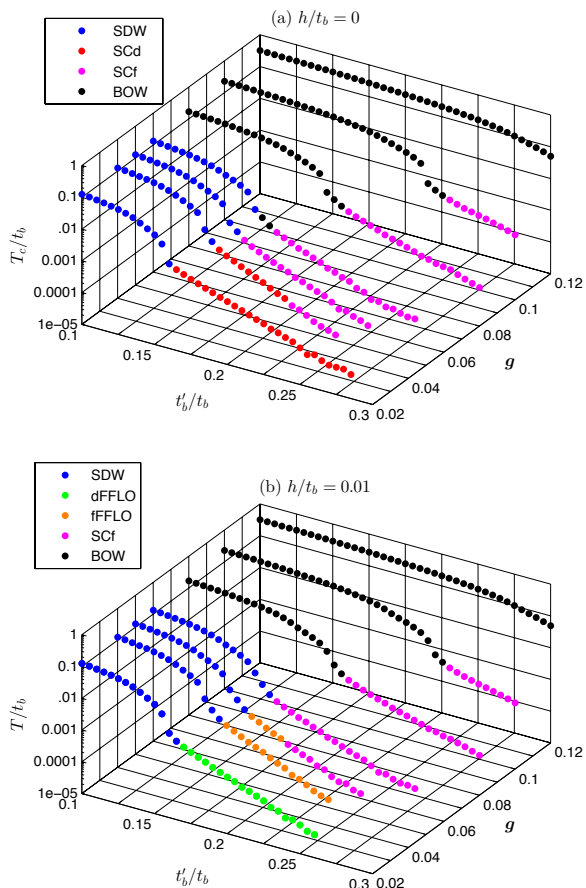


FIG. 5. Phase diagram of the extended quasi-electron gas model at (a): $h = 0$, and (b): $h/t_b = 0.01$.

ing. This sequence is soon modified by the incursion of a BOW instability from (12) in the sequence near t'_b^* , as shown in Fig. 5 (a). By increasing further \mathbf{g} , near 0.1, makes the SDW unstable and yields the sequence BOW \rightarrow SCf. This is also associated with the smearing of the quantum critical region to the benefit of the BOW ordering. Apart from few details at the quantitative level, the present results confirm those of Nickel *et al*²⁰.

If we now switch on the effect of magnetic field, we observe that the range of influence of triplet superconductivity is enlarged along the \mathbf{g} axis. Thus from $\mathbf{g} \simeq 0.04$ and for $h/t_b \gtrsim 0.004$, the dFFLO state of Fig. 1 becomes unstable against the formation of a triplet fFFLO, $S_z = 0$, state governed by the divergence of (18), as shown in Fig. 2 (b) at $\mathbf{g} = 0.04$. The related combination of couplings $g_{2\perp}(k'_b, -k'_b, k_b) - g_{1\perp}(k'_b, -k'_b, k_b)$ in the $k'_b k_b$ plane is plotted in Fig. 6 (a) close to $T_c(h)$. One observes pronounced modulations in momentum space compatible with $f_{\text{fFFLO}} = \sqrt{2} \cos k_b^{(l)}$ and peaks at $k_b^{(l)} = 0, \pm\pi$, along the lines $k'_b = -k_b \pm \pi$, which results mainly from SDW scattering. According to Fig. 2 (b), in this range of \mathbf{g} , SDW correlations are by far dominant down to very close to $T_c(h)$ and act as the main source of interchain

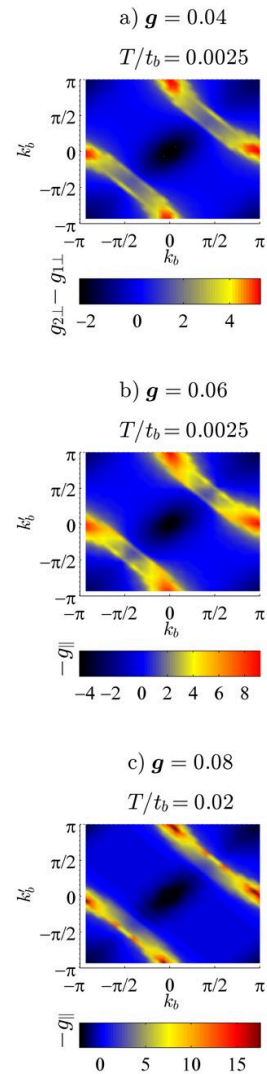


FIG. 6. Low temperature effective scattering amplitudes close to T_c in the momentum space at $h/t_b = 0.01$, for: (a) $g_{2\perp}(k'_b, -k'_b, k_b) - g_{1\perp}(k'_b, -k'_b, k_b)$ for fFFLO ; (b) and (c) $g_{\parallel}(k'_b, -k'_b, k_b)$ for SCf₁.

pairing for the fFFLO state at $S_z = 0$. It is worth mentioning that its existence has not been reported from mean-field theory analysis³⁴. However, the FFLO mixing with triplet superconductivity has been found from this analysis and from DMRG in the two-legs ladders systems at strong coupling⁵⁵.

When \mathbf{g} further increases to reach $\mathbf{g} \simeq 0.05$, the fFFLO state becomes in turn unstable to the benefit of uniform triplet SCf₁ state at $S_z = 1$, and a sequence of instabilities, SDW \rightarrow SCf₁ along t'_b , as indicated in Fig. 5 (b). This sequence in the above \mathbf{g} range is similar to the one found in Fig. 5 (a) in the absence of field. Following (16), the SCf₁ pairing is directly connected to the combination of couplings $g_{\parallel}(k'_b, -k'_b, k_b)$ for parallel spins. From Fig. 6 (b), g_{\parallel} presents strong modulations in the $k'_b k_b$

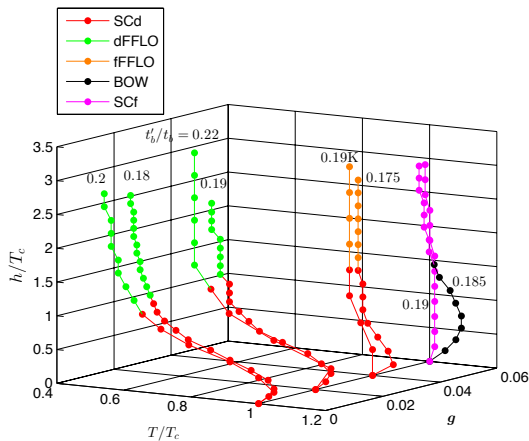


FIG. 7. The evolution of h_{c2} vs temperature for various t'_b and as a function of interchain coupling \mathbf{g} .

plane near $T_c(h)$, which are consistent with the form factor $f_{\text{SCf}} = \sqrt{2} \cos k'_b$. As meant by the couplings involved in the BOW susceptibility in (12), peaks along the lines $k'_b = -k_b \pm \pi$ are consistent with the presence of strong BOW correlations which acts as the main source of SCf_1 pairing^{18,20,35}. As displayed in Fig. 2 (b), the amplitude of BOW correlations are close in amplitude to SDW.

At $\mathbf{g} \gtrsim 0.08$, the SDW state becomes in its turn unstable at low t'_b in favour of a BOW state and the sequence $\text{BOW} \rightarrow \text{SCf}_1$ as a function of t'_b . The importance of BOW growth at the expense of SCf along the \mathbf{g} axis, as found in the absence of field [Figs 5 (a) and (b)]. This is reflected in Fig. 6 (c) for the modulation of the relevant coupling, g_{\parallel} , for SCf_1 in the $k'_b k_b$ plane, which is less pronounced on the negative side.

It is instructive to trace the temperature dependence of the critical field $h_{c2}(T)$ for the above selected ranges of interchain coupling \mathbf{g} . At very low \mathbf{g} , the Fig. 7 shows that under field, we have the expected sequence of instabilities $\text{SCd} \rightarrow \text{dFFLO}$ previously found in Fig. 4 at $\mathbf{g} = 0$. The violation of the Pauli limit in the dFFLO regime is dependent on antinesting and is reduced upon increasing t'_b . At higher \mathbf{g} , when fFFLO becomes possible, the crossover of SCd to fFFLO under field is much more rapid and the violation of the Pauli limit, consequently more pronounced, with an almost vertical upturn of h_{c2} . Increasing further \mathbf{g} , the vertical rise of the h_{c2} line for SCf_1 does not lead to a crossover to another state, except for t'_b close to the junction with BOW order, where one can start with a BOW state at low field and which is followed at sufficiently high field by a reentrant triplet SCf_1 state.

By way of closing the section, we give in Fig. 8 the phase diagram in the $\mathbf{g}h$ plane which displays the transformation of ordered phases under magnetic field when the interchain interaction is varied at a fixed t'_b in the superconducting sector at $\mathbf{g} = 0$. From the Figure, we observe that for a sizeable interval of weak repul-

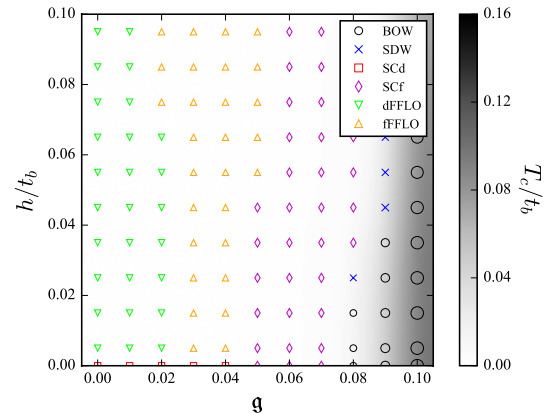


FIG. 8. The phase diagram in the $\mathbf{g} - h$ plane for $t'_b/t_b = 0.2$.

sive \mathbf{g} , the possible modifications of superconductivity expands under magnetic field to the benefit of FFLO states. These are not exclusively restricted to the d -wave sector, but also belong to the triplet f -wave sector at $S_z = 0$. Thus at relatively weak interchain repulsion, the sequences $\text{SCd} \rightarrow \text{dFFLO}$, $\text{SCd} \rightarrow \text{dFFLO} \rightarrow \text{fFFLO}$ and $\text{SCd} \rightarrow \text{fFFLO}$ are possible transformations of superconductivity within an accessible range of magnetic field ($h/t_b < 0.1$). It is worth noting that no $\text{SCd} \rightarrow \text{SCf}$ transition, from singlet to triplet uniform superconductivity, is predicted under field over all the range of \mathbf{g} covered, this at variance with previous mean-field results³⁴. Furthermore, as previously discussed for stronger interchain interaction, namely when instead of superconductivity, a BOW order is favoured in zero field, the sequences $\text{BOW} \rightarrow \text{SCf}$ and $\text{BOW} \rightarrow \text{SDW}_{xy} \rightarrow \text{SCf}$ can be found showing the stabilization of uniform SCf from density-wave phases under sufficiently high magnetic field.

V. SUMMARY AND CONCLUDING REMARKS

In this work we employed the weak coupling renormalization group method to examine the possible instabilities of the extended quasi-1D electron gas model with half-filling umklapp scattering and the presence of a magnetic field. The field is Zeeman coupled to spin degrees of freedom exclusively, which simulates the weakness of orbital pair breaking effect that characterizes specific planar field orientations in low dimensional superconductors like the Bechgaard salts.

For purely intrachain repulsive interactions, the SCd state of the electron gas is suppressed under field, evolving toward inhomogeneous d -wave FFLO superconductivity rather than uniform triplet superconductivity. The dFFLO state is accompanied by a violation of the Pauli limiting field H_P for singlet superconductivity, which is particularly enhanced by the constructive quantum interference between Cooper pairing and antiferromagnetic

fluctuations. The enhancement is then found to scale in a non universal way with both the interaction and the distance to the quantum critical point joining superconductivity and the spin-density-wave state in the phase diagram. These results obtained in the presence of half-filling umklapp scattering broaden the impact of an earlier study made at incommensurate band filling⁴¹.

For the extended version of the quasi-electron electron gas model when interchain Coulomb interaction is included and a transition from d-wave to triplet f -wave superconductivity becomes possible. We find that its range of stability is somewhat enlarged by the magnetic field as one moves along the axis of interchain repulsion. The calculations reveal the existence of an intermediate f -wave FFLO state of zero total spin projection, which emerges within a finite interval of interchain Coulomb repulsion interaction before the onset of uniform f -wave superconductivity.

The possible field-induced FFLO states obtained provide an interesting avenue of interpretation for the persistent superconductivity in resistivity experiments observed well above the Pauli limiting field of the Bechgaard salts when they are very close to their quantum critical point. The results also allow the possibility for a direct experimental test of the theory from future resistivity experiments that would be conducted on a large pressure interval, in order to check if the anomalous enhancement of the upper critical field is suppressed in the limit of high pressure, as predicted⁴¹. Existing resistivity

data on a $(\text{TMTSF})_2\text{PF}_6^{54}$, though obtained in a limited range of pressures close to the critical value, head in this direction.

From the renormalization group viewpoint developed in the present work, it is not clear a priori which one of the d and f FFLO states is likely to be more favorable in systems like the Bechgaard salts. Both phases are occurring relatively close one another and both are falling in a reasonable range of parameters for these materials. It must be said, however, that the currently observed violation of the Pauli limit in the Bechgaard salts is significantly less pronounced than predicted in the triplet case. This would in turn tip the balance in favour of the singlet dFFLO scenario for the high field superconducting phase in the Bechgaard salts.

ACKNOWLEDGMENTS

We thank Samuel Desrosiers for his help on computational aspects of this work. C.B. thanks the National Science and Engineering Research Council of Canada (NSERC) under Grant No. RGPIN-2016-06017, and the Réseau Québécois des Matériaux de Pointe (RQMP) for financial support. Simulations were performed on computers provided by Canadian Foundation for Innovation, the Ministère de l'Éducation des Loisirs et du Sport (Québec), Calcul Québec, and Compute Canada.

-
- ¹ D. Jérôme, A. Mazaud, M. Ribault, and K. Bechgaard, *J. Phys. (Paris) Lett.* **41**, L95 (1980).
- ² D. Jérôme and H. J. Schulz, *Adv. Phys.* **31**, 299 (1982).
- ³ N. Doiron-Leyraud, P. Auban-Senzier, S. René de Cotret, C. Bourbonnais, D. Jérôme, K. Bechgaard, and L. Taillefer, *Phys. Rev. B* **80**, 214531 (2009).
- ⁴ V. J. Emery, *Synth. Met.* **13**, 21 (1986).
- ⁵ M. T. Béal-Monod, C. Bourbonnais, and V. J. Emery, *Phys. Rev. B* **34**, 7716 (1986).
- ⁶ L. G. Caron and C. Bourbonnais, *Physica B + C* **143**, 453 (1986).
- ⁷ D. J. Scalapino, E. Loh, and J. E. Hirsch, *Phys. Rev. B* **34**, R8190 (1986).
- ⁸ C. Bourbonnais and L. G. Caron, *Europhys. Lett.* **5**, 209 (1988).
- ⁹ M. Takigawa, H. Yasuoka, and G. Saito, *J. Phys. Soc. Jpn* **56**, 873 (1987).
- ¹⁰ Y. Hasegawa and H. Fukuyama, *J. Phys. Soc. Jpn.* **56**, 877 (1987).
- ¹¹ M.-Y. Choi, P. Chaikin, S. Z. Huang, P. Haen, E. M. Engler, and R. L. Greene, *Phys. Rev. B* **25**, 6208 (1982).
- ¹² S. Tomic, D. Jerome, D. Mailly, M. Ribault, and K. Bechgaard, *J. Phys. (Paris) Coll.* **44**, C31075 (1983).
- ¹³ C. Coulon, P. Delhaes, J. Amiel, J. P. Manceau, J. M. Fabre, and L. Giral, *J. Phys. (Paris)* **43**, 1721 (1982).
- ¹⁴ N. Joo, P. Auban-Senzier, C. R. Pasquier, D. Jérôme, and K. Bechgaard, *Europhys. Lett.* **72**, 645 (2005).
- ¹⁵ S. Belin and K. Behnia, *Phys. Rev. Lett.* **79**, 2125 (1997).
- ¹⁶ F. L. Pratt, T. Lancaster, S. J. Blundell, and C. Baines, *Phys. Rev. Lett.* **110**, 107005 (2013).
- ¹⁷ A. A. Abrikosov, *J. Low Temp. Phys.* **53**, 359 (1983).
- ¹⁸ K. Kuroki, R. Arita, and H. Aoki, *Phys. Rev. B* **63**, 094509 (2001); S. Onari, R. Arita, K. Kuroki, and H. Aoki, *Phys. Rev. B* **70**, 094523 (2004); Y. Tanaka and K. Kuroki, *Phys. Rev. B* **70**, 0605502(R) (2004).
- ¹⁹ Y. Fuseya and Y. Suzumura, *J. Phys. Soc. Jpn.* **74**, 1263 (2005).
- ²⁰ J. C. Nickel, R. Duprat, C. Bourbonnais, and N. Dupuis, *Phys. Rev. Lett.* **95**, 247001 (2005); *Phys. Rev. B* **73**, 165126 (2006).
- ²¹ I. J. Lee, S. Brown, W. G. Clark, M. J. Strouse, M. J. Naughton, W. Kang, and P. M. Chaikin, *Phys. Rev. Lett.* **88**, 17004 (2002).
- ²² R. Brusetti, M. Ribault, D. Jerome, and K. Bechgaard, *J. Phys. (Paris)* **43**, 801 (1982).
- ²³ L. P. Gorkov and D. Jérôme, *J. Phys. Lett.* **46**, L643 (1985).
- ²⁴ I. J. Lee, M. J. Naughton, G. M. Danner, and P. M. Chaikin, *Phys. Rev. Lett.* **78**, 3555 (1997).
- ²⁵ I. J. Lee, A. P. Hope, M. J. Leone, and M. J. Naughton, *Synth. Met.* **70**, 747 (1995).
- ²⁶ I. J. Lee, P. M. Chaikin, and M. J. Naughton, *Phys. Rev. B* **62**, R14669 (2000).
- ²⁷ A. G. Lebed, *JETP Lett.* **44**, 114 (1986).
- ²⁸ N. Dupuis, G. Montambaux, and C. A. R. S. de Melo, *Phys. Rev. Lett.* **70**, 2613 (1993).

- ²⁹ J. Shinagawa, Y. Kurosaki, F. Zhang, C. Parker, S. E. Brown, D. Jérôme, K. Bechgaard, and J. B. Christensen, *Phys. Rev. Lett.* **98**, 147002 (2007).
- ³⁰ H. Shimahara, *Phys. Rev. B* **61**, R14936 (2000).
- ³¹ N. Belmechri, G. Abramovici, M. Heritier, S. Haddad, and S. Charfi-Kaddour, *EPL* **80**, 37004 (2007).
- ³² N. Belmechri, G. Abramovici, and M. Heritier, *EPL* **82**, 47009 (2008).
- ³³ H. Aizawa, K. Kuroki, and Y. Tanaka, *Phys. Rev. B* **77**, 144513 (2008).
- ³⁴ H. Aizawa, K. Kuroki, T. Yokoyama, and Y. Tanaka, *Phys. Rev. Lett.* **102**, 016403 (2009).
- ³⁵ K. Kajiwara, M. Tsuchiizu, Y. Suzumura, and C. Bourbonnais, *J. Phys. Soc. Jpn.* **78**, 104702 (2009).
- ³⁶ A. G. Lebed, *Phys. Rev. Lett.* **107**, 087004 (2011).
- ³⁷ S. Yonezawa, S. Kusaba, Y. Maeno, P. Auban-Senzier, C. Pasquier, K. Bechgaard, and D. Jerome, *Phys. Rev. Lett.* **100**, 117002 (2008).
- ³⁸ S. Yonezawa, S. Kusaba, Y. Maeno, P. Auban-Senzier, C. Pasquier, and D. Jerome, *J. Phys. Soc. Jpn* **77**, 054712 (2008).
- ³⁹ S. Yonezawa, Y. Maeno, K. Bechgaard, and D. Jerome, *Phys. Rev. B* **85**, 140502(R) (2012).
- ⁴⁰ D. Jérôme and S. Yonezawa, *C. R. Physique* **17**, 357 (2016).
- ⁴¹ Y. Fuseya, C. Bourbonnais, and K. Miyake, *Europhys. Lett.* **100**, 5708 (2012).
- ⁴² V. J. Emery, R. Bruinsma, and S. Barisic, *Phys. Rev. Lett.* **48**, 1039 (1982).
- ⁴³ C. Bourbonnais and A. Sedeki, *Phys. Rev. B* **80**, 085105 (2009).
- ⁴⁴ A. Sedeki, D. Bergeron, and C. Bourbonnais, *Phys. Rev. B* **85**, 165129 (2012).
- ⁴⁵ M. Shahbazi and C. Bourbonnais, *Phys. Rev. B* **92**, 195141 (2015).
- ⁴⁶ M. Shahbazi and C. Bourbonnais, *Phys. Rev. B* **94**, 195153 (2016).
- ⁴⁷ L. P. Gor'kov and I. E. Dzyaloshinskii, *Sov. Phys. JETP* **40**, 198 (1974).
- ⁴⁸ P. M. Grant, *J. Phys. (Paris) Coll.* **44**, C3847 (1983).
- ⁴⁹ L. Ducasse, A. Abderrabba, J. Hoarau, M. Pesquer, B. Gallois, and J. Gaultier, *J. Phys. C* **19**, 3805 (1986).
- ⁵⁰ P. Wzietek, F. Creuzet, C. Bourbonnais, D. Jerome, K. Bechgaard, and P. Batail, *J. Phys. I* **3**, 171 (1993).
- ⁵¹ S. Barisic and S. Brazovskii, in *Recent Developments in Condensed Matter Physics*, Vol. 1, edited by J. T. Devreese (Plenum, New York, 1981) p. 327.
- ⁵² K. Penc and F. Mila, *Phys. Rev. B* **50**, 11 429 (1994).
- ⁵³ Y. Matsuda and H. Shimahara, *J. Phys. Soc. Jpn.* **76**, 051005 (2007).
- ⁵⁴ I. J. Lee, M. J. Naughton, and P. M. Chaikin, *Phys. Rev. Lett.* **88**, 207002 (2002).
- ⁵⁵ G. Roux, S. White, S. Capponi, and D. Poilblanc, *Phys. Rev. Lett.* **97**, 087207 (2006).